IEEE Access
Multidisciplinary | Rapid Review | Open Access Journal

Received February 2, 2019, accepted February 27, 2019, date of publication March 1, 2019, date of current version April 5, 2019.

*Digital Object Identifier 10.1109/ACCESS.2019.2902543*

# "Light in and Sound Out": Review of Photoacoustic Imaging in Cardiovascular Medicine

**DA-YA YANG[1,2], YUAN ZHU[3], JIAN-QIU KONG[3], XIAO-JING GONG[4], ZHI-HUA XIE[4], WEI-YI MEI[1,2], CHU-FAN LUO[1,2], ZHI-MIN DU[1,2], XIAO-DONG ZHUANG[1,2], AND XIN-XUE LIAO[1,2]**

[1]Department of Cardiology, The First Affiliated Hospital, Sun Yat-sen University, Guangzhou 510080, China
[2]NHC Key Laboratory of Assisted Circulation, Sun Yat-sen University, Guangzhou 510080, China
[3]Zhongshan School of Medicine, Sun Yat-sen University, Guangzhou 510080, China
[4]Research Laboratory for Biomedical Optics and Molecular Imaging, Shenzhen Institutes of Advanced Technology, Chinese Academy of Sciences, Shenzhen 518172, China

Corresponding authors: Xiao-Dong Zhuang (zhuangxd3@mail.sysu.edu.cn) and Xin-Xue Liao (liaoxinx@mail.sysu.edu.cn)

This work was supported in part by the Shenzhen Science and Technology Innovation Grant under Project JCYJ20160608214524052, in part by the Science and Technology Planning Project of Guangdong Province under Project 2016A020220007 and Project 2014B050505013, and in part by the National Natural Science Foundation of China under Project 61475182 and Project 81427804.

**ABSTRACT** Photoacoustic imaging (PAI) is one of the most recent additions to the expanding armamentarium of diagnostic imaging technologies. Based on the working principles of optics and ultrasound, PAI provides relatively accurate, differential, and comprehensive information for a variety of physiological and pathological conditions in a real-time fashion. PAI was previously put to use in the field clinical oncology and has only recently been attempted in diseases of the heart and vessels. Notwithstanding the fact that it is still in the pre-clinical stage, PAI, with its important advances, has shown considerable potential to make a significant, transformative leap forward in cardiovascular imaging. The applications of PAI-based techniques in cardiovascular medicine include, but are not limited to, the identification and evaluation of atherosclerotic vulnerable plaque (with or without the use of tissue-specific extraneous contrast), the visualization of clots in different thrombosis-related diseases, the detection of myocardial lesions during catheter ablation of cardiac arrhythmias, the real-time monitoring of blood rheology and hemodynamics, and so on. In this contemporary literature review, we have summarized major applications of different PAI-based techniques for various cardiovascular situations, highlighted key innovations, and their respective clinical feasibilities, and then discussed future perspectives of these versatile methodologies in the practice of cardiovascular imaging. In our view, the unique advantages of PAI render it immensely promising to open up new avenues in the study of cardiovascular diseases.

**INDEX TERMS** Photoacoustic imaging, cardiovascular disease, spectroscopy.

## I. INTRODUCTION

Due to the heterogeneous clinical features and complex pathologic mechanisms of cardiovascular diseases, obtaining clinically relevant morphological and pathological information in an unambiguous, comprehensive, time-sensitive and cost-effective manner, remains a major challenge for both clinicians and research scientists. Currently, many novel imaging modalities are under intense ex vivo and in vivo investigations [1]–[4]. Among these, photoacoustic imaging (PAI), also known as optoacoustic tomography [5], is a promising tool to be applied in multiple clinical situations.

Ingeniously encapsulated as "*light in and sound out*" [6], PAI technique combines working principles of both optical and ultrasound imaging. Detailed explanations of PAI basics have been timely covered elsewhere [7], [8]. In brief, with low-energy and short pulses of laser light irradiating, broadband waves are generated through optical absorption and associated thermoelastic expansion, subsequently creating photoacoustic waves that can be captured by an ultrasound

The associate editor coordinating the review of this manuscript and approving it for publication was Tao Zhou.

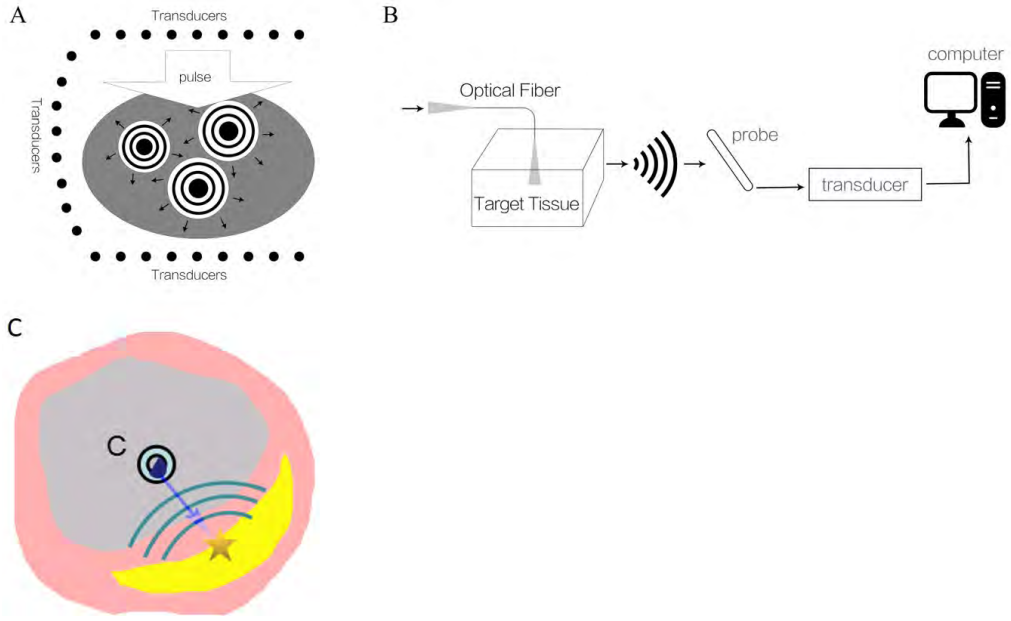


**FIGURE 1.** Sketch of the photoacoustic imaging (PAI) principle. A. Under short-pulse laser irradiation, target tissue is able to expand due to thermal absorption. Broadband acoustic wave is generated by the conversion of light energy to thermal and mechanical stress. B. An ultrasonic transducer on photoacoustic imaging catheter is used to receive photoacoustic signal from the target tissue. Real-time imaging through computer algorithm is subsequently reconstructed in silico. C. The catheter (C) generates a laser pulse (soft blue) to the plaque (yellow) in the vessel wall. Then, an acoustic wave (green) is produced by thermoelastic expansion (wheat color) and photoconversion from light excitation.

detector (Figure. 1) [8]. Hence, PAI combines the advantages of optical imaging, namely, high contrast and spectroscopic specificity, with the advantages of ultrasound imaging, namely, high spatial resolution and penetration depth. Before, PAI has been used predominately in the field of oncology. Its application in cardiovascular diseases is attempted by researchers only recently [3]. Of note, PAI enables various new invasive or non-invasive approaches in cardiovascular medicine for diagnostic purposes, which include, but are not limited to, discrimination between different tissue types, detection of vulnerable plaques with or without additional target-specific molecular probes, the visualization of clots in different thrombosis-related diseases, guidance for interventional decision-making, real-time monitoring of blood rheology and hemodynamics, and so on.

In this review, we will systematically examine current literature apropos of the applications of PAI in basic sciences and pre-clinical studies, according to its intravascular and non-vascular usage, by selected pathological and pathophysiological entities. We will then move on to briefly discuss its future role in cardiovascular medicine.

## II. INTRAVASCULAR PHOTOACOUSTIC IMAGING

### A. VULNERABLE PLAQUE

The rupture of vulnerable atherosclerotic plaques and subsequent thrombosis is well recognized to be the initiator of acute cardiovascular events and, possibly, sudden cardiac death [9], [10]. Although the atherosclerotic plaque can be identified by traditional imaging modalities such as angiography and intravascular ultrasound (IVUS), these techniques fall short in accurately evaluating its biological composition and anatomical structure, which have been shown to be the determining factors of plaque vulnerability [11]–[14]. By harnessing light and sound and creating more favorable spatial resolution and penetration depth, intravascular photoacoustic (IVPA) imaging technique takes a giant leap forward in accurately identifying morphology and components of a plaque [3], [4], [7], [15]. During IVPA imaging, atherosclerotic plaques are visualized according to different optical absorption characteristics of various tissue components (Figure. 2) [16]. In a recent study, IVPA was shown to be comparable with Near-Infrared Spectroscopy (NIRS) in its sensitivity to quantify and localize lipid within atherosclerotic plaques, yet at the same time provides additional depth resolution, for which NIRS itself is deficient [17]. A brief summary comparing two intravascular imaging techniques currently in clinical use with PAI is shown in Table 1.

Based on distinct optical absorption spectrum, IVPA imaging can assess components of and changes in the atherosclerotic artery against normal surrounding tissues [7], [18]. In one study, samples of human atherosclerotic aorta were visualized in vitro at 461 and 532 nm contrasted with lipids and 308 nm contrasted with calcium [19], [20]. Of note, high absorption of blood is an important obstacle to identifying normal and athermanous areas across arterial tissues in the visible range [7]. However, in the near infrared (NIR) wavelength range, blood absorption is much lower over 680–1300 nm, while lipid absorption peaks

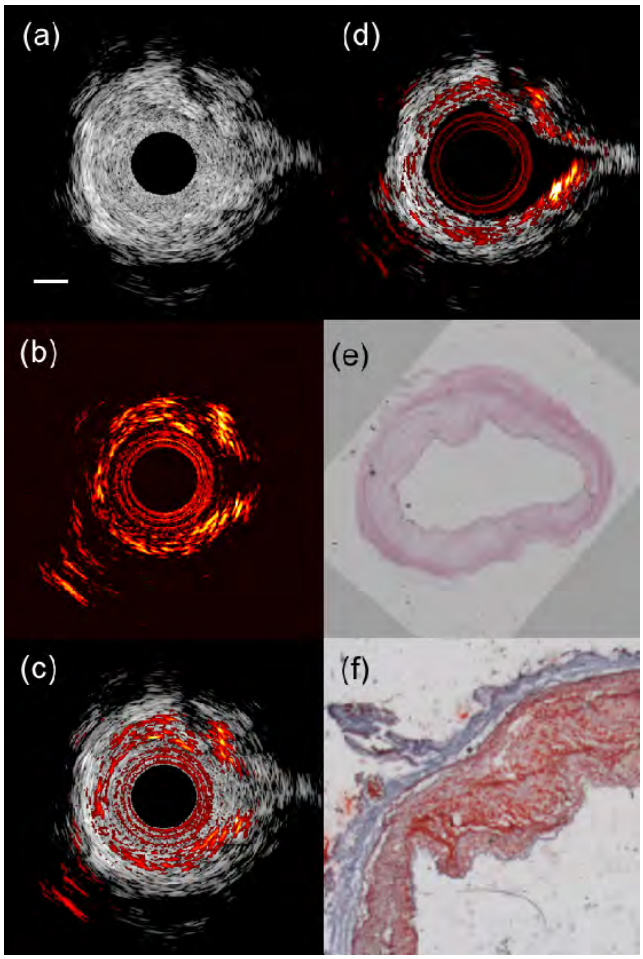


**FIGURE 2.** (a) IVUS, (b) IVPA, and (c) combined IVUS/IVPA images of an atherosclerotic rabbit aorta acquired in the presence of blood. (d) Combined IVUS/IVPA image of the same cross section of the aorta imaged in saline. The scale bar is 1 mm. (e) H&E and (f) Oil red O stain of the tissue slice adjacent to the imaged tissue cross section indicate that the aorta has lipid-rich plaque16. Reproduced with permission. Courtesy from Stanislav Emelianov. (Ref. 16).

around 1210 nm [21]. Therefore, lipid-rich collagen type I and collagen type III can be identified through differences in spectral slopes between normal and atherosclerotic arteries, as one study has shown using rabbits aorta samples ex vivo [7]. In another study, the same 1720 nm single wavelength (at which the absorption coefficient is high for lipids while low for blood and water) was used in a hypercholesterolemic rabbit model through in vivo IVPA, which for the first time demonstrated the possibility to obtain IVPA images without flushing blood from the artery [18].

The first ex vivo IVPA imaging of human atherosclerotic coronary arteries was reported in 2011 [22]. The distinct imaging of lipids was processed by spectroscopic imaging over 715–1400 nm, and the absorption spectrum peaks around 1210 nm. As a result, this specific peak value is used in subsequent studies to identify lipids from other tissue components of the vessel wall. Jansen *et al.* used co-registered cross-sectional IVPA/IVUS scans of fresh ex vivo human coronary arteries from 1185–1235 nm at 10 nm intervals and demonstrated that IVPA imaging could detect and differentiate lipids in the atherosclerotic plaque from those in the peri-adventitial area at three different wavelengths [23]. In another study, IVPA imaging of human coronary atherosclerosis was also achievable at 1720 nm [18]. Both 1.2 mm and 1.7 mm wavelength bands are considered to be suitable for imaging lipids in atherosclerosis. However, IVPA could only differentiate plaque and peri-adventitial lipids at 1.2 mm [24]. In addition, in another ex vivo study, Arabul *et al.* reported the accurate detection of intraplaque hemorrhage in human carotid plaque samples, the majority of which were not visible by ultrasound, adding another layer of advantage of PAI-based imaging in assessing plaque vulnerability [25].

Furthermore, in IVPA imaging, exogenous absorbers can be introduced to the plaque/lesion in order to provide extra information at the molecular or cellular levels. For example, macrophages are suitable imaging targets at all developmental stages of atherosclerosis [26]. These cells cannot provide endogenous contrast themselves but can be visualized by adding a contrast agent. There are currently quite a number of available contrast agents. Gold nanoparticles (AuNPs), known by their favorable biocompatibility and high optical scattering coefficients, have been proven to be one of the many excellent choices [27]–[29]. The individual spherical nanoparticles' peak is at 530 nm wavelength with a weak photoacoustic signal at 680 nm [30]. However, after being endocytosed by macrophages, the gold nanoparticles aggregate with a shifted peak in the absorption spectrum compared with their extracellular counterparts. At 700 nm wavelength, the aggregated gold nanoparticles produce the strongest PA signal (also known as the plasmon resonance coupling effect). For this reason, the imaging contrast is presumed to be enhanced by high local concentration of gold nanoparticles absorbed in macrophages. This theory has been tested by injecting macrophages loaded with gold nanoparticles in the atherosclerotic rabbit aorta in vivo [30]. In the same study, IVPA has also been shown to be able to identify the location of acute inflammation within atherosclerotic plaques, due to the tendency of the gold nanoparticles to extravasate at sites with dysfunctional endothelium, i.e., regions with compromised luminal endothelium and acute inflammation. Yeager's study repeated the same result of IVPA imaging in ex vivo settings [31]. In addition, nanoparticles can be modified chemically to reduce cytotoxicity as well as increase stability and circulation time [6], [32]. For example, the layer of silica coating can improve the stability of the nanoparticles and maintain their original shape for an extended period of time. Also, in the near-infrared wavelength range, silica-coated nanoparticles' IVPA signal intensity and temperature are proved to be linearly correlated, the slope of which is greater than that of endogenous tissues [33]. Therefore, such processing has the potential to enable precise detection and temperature monitoring of atherosclerotic plaques through selective heating of plasmonic gold nanoparticles.

Matrix metalloproteinase (MMP), secreted by macrophages, acts to weaken the fibrous cap, causing the plaques to

**TABLE 1.** Brief comparison of OCT, IVUS and PAI techniques.

| Imaging Modalities | Optical Coherence Tomography (OCT) | Intravascular Ultrasound (IVUS) | Photoacoustic Imaging (PAI) |
|---|---|---|---|
| Type of radiation | Near-infrared light | Ultrasound | (Near-Infrared) Light + Ultrasound |
| Axial resolution (μm) | 100-200 | 10-15 | 100 |
| Lateral resolution (μm) | 300-500 | 30-40 | 400-50 |
| Penetration (mm) | 10 | 1 | 5 |
| Contract mechanism | Acoustic scattering | Optical scattering | Optical absorption |
| Current status | CS/CA | CS/CA | PCS |
| Excellent assessment | Lumen area, Plaque rupture | Lumen area, plaque burden, positive remodeling, calcium | Necrotic core |
| Good assessment | Fibrous-cap thickness, TCFA, erosion, thrombus, calcium | Plaque rupture | NA |
| Possible assessment | inflammation | Necrotic core, thrombus | Lumen area, plaque burden, positive remodeling, |
| Impossible assessment | Plaque burden, positive remodeling, Necrotic core | Fibrous-cap thickness, TCFA, erosion, inflammation | Fibrous-cap thickness, plaque rupture, erosion, thrombus, calcium |

CA=clinically, commercially available; CS=clinical studies; PCS=pre-clinical studies; TCFA=thin-cap fibroatheroma

be more inclined to rupture. As a result, MMP is emerging as an important modulator of atherothrombosis [9], [34], the activity of which can be detected by the Near-Infrared Fluorescence (NIRF) emitting probes in plaques. As an MMP-sensitive activatable fluorescent probe, MMPSense680 is able to fluoresce based on the proteolytic cleavage by MMP [35], [36]. It can also be activated by a broad range of MMP subtypes, including MMP 2, 3, 9, and 13 [36]. Upon activation, it will undergo changes in light absorption. Moreover, it produces a much lower PA signal intensity than gold nanoparticles due to their lower absorption [7]. MMPSense 680 was also applied to provide volumetric mapping of the vulnerable plaques in human carotid artery samples excised from symptomatic patients [37]. A recent animal study had successfully used gold nanorods conjugated with MMP2 antibody for in vivo quantitative detection of MMP2 in atherosclerotic plaques of rabbits [38].

Indocyanine green (ICG), an intravenous tricarbocyanine dye, has the unique properties of near-infrared absorption with molecular and cellular targets relevant to atherosclerosis, such as low-density and high-density lipoproteins [39]–[41] With maximum absorption at 785 nm in aqueous solutions and 805 nm in blood, ICG has been used for the identification of lipid-rich, inflamed atheroma and macrophages in vivo [40], [42], [43]. ICG can be another excellent contrast agent to detect atherosclerosis, as an in vitro study showed that spatial distribution and structural information of ICG-labeled macrophages could be presented clearly with high contrast and sensitivity by IVPA/IVUS imaging [44].

Of note, IVPA imaging is often synergistically combined with IVUS imaging due to common hardware components such as ultrasound transducer and electronic receiver [4]. Herein, combining these two imaging modalities can obtain both functional and anatomical information about the tissue of interest. Several prototypes for hybrid IVUS-IVPA imaging had been successfully developed [45], [46]. In addition, the fusion of IVPA and OCT is a feasible option, also [47], [48].

### *B. THROMBOSIS*

In situ thrombosis is one of the key pathophysiological processes in acute myocardial infarction and ischemic stroke. Besides that, dislodged blood clots (e.g., from left atrial appendage in atrial fibrillation) can also cause thromboembolism and vascular occlusion [49]. The so-called negative PA contrast indicates that signals from the targets are below background, possibly resulting from the thermodynamic sample temperature or additional absorption [50]. Zharov *et al.* had previously found the effect of kinetic cooling, with the manifestation of negative PA signals in CO2 + N2 mixture

under CO2 pulse laser [51], which can be explained by the fact that thermodynamic (i.e., Boltzmann) energy deficit of the depleted low-energy levels is quickly taking from the kinetic energy. As mentioned above, the high-absorbing hemoglobin in RBCs demonstrates a high PA background, which can traditionally mask the absorption of targets of interest, necessitating a higher absorption compared with blood. Using negative contrast PA imaging, researchers can visualize an ultra-sharp negative PA hole in the background of blood due to a decrease in regional absorption [50], [52]. Therefore, multiple clots including white, red and mixed clots can be identified, including concentration and size of clots (even as small as 20 $\mu$m) [50], [52]. However, a technical difficulty has to be solved before complete visualization of a vessel becomes possible, namely, the appropriate selection of correct laser geometry. In summary, PAI holds great promise to be used for clot detection, in that it provides useful information in diagnosing and prognosticating clot-induced diseases such as myocardial infarction and stroke.

## III. NONVASCULAR PHOTOACOUSTIC IMAGING

Nonvascular applications of photoacoustic imaging in cardiovascular medicine include guidance for arrhythmia ablation, evaluation of cardiovascular hemodynamics and so on.

### A. ABLATION OF CARDIAC ARRHYTHMIA

Cardiac arrhythmia is a common and particular type of cardiovascular diseases, among which atrial fibrillation (AF) is one of the most common arrhythmias encountered in clinical practice, with an estimated number of over 2 million patients affected worldwide [49]. AF is associated with an increased risk of stroke [53]–[55], dementia, heart failure [56], and so forth. The treatment of AF is still largely unsatisfactory because reoccurrence rate after anti-arrhythmic treatment remains as high as 25% [57]. Conventional ''rhythm control'' strategy for AF includes pharmacologic therapy and radiofrequency trans-catheter ablation, with the latter being the more effective option [58]. Nevertheless, one of the limiting factors of ablation therapy is its inability of evaluating and monitoring the durability and transmurality of lesion. The therapeutic effects of catheter-based ablation can be altered by, among other factors, catheter contact force, radiofrequency energy parameters and varying experiences of physicians [58]. Moreover, the disturbing prospect of severe complications such as atrio-esophageal fistulae and cardiac tamponade calls for the introduction of new methods for clearly imaging the ablation site in real time [59]. Various imaging methods have been tried, including MRI, optical coherence tomography (OCT) and acoustic radiation force impulse (ARFI). MRI has an inadequate spatial resolution and frame rates and is also to be blamed for its high costs as well as extended time for imaging. OCT is a relatively new method but falls short in this case due to its inability to penetrate thick tissues [60]. ARFI may be useful through interrogating mechanical features of the heart but is causing too many artifacts to be precise [61].

The photoacoustic method is capable of imaging the ablation lesion in real time and with convenience. N Dana *et al.* reported the combination of ultrasound (US) and spectroscopic photoacoustic (sPA) imaging to characterize the effect of ablation on an excised fresh porcine heart [62]. They acquired a single 3-D combined PA/US B-mode scan on each sample at 710 nm, from which a 2-D plane of the brightest region of PA signal was used to construct sPA imaging. After that, the frames were averaged to create a single image. As previous studies reported, the hemoglobin (Hb) was the primary absorber in an oxygen-deficient myocardial sample, resulting in an outstanding hump near 760 nm [63]. The non-ablated absorption spectrum correlates well with that of Hb, and the ablated absorption spectrum decreases monotonically [63]. Based on these data, a 3-D TCM (tissue characterization map)/US data was constructed to visualize the 3-D scene of the ablation lesion better. As the results obtained by the photoacoustic technique showing high consistency with that of gross pathology, sPA imaging is able to identify the ablated and non-ablated myocardium accurately and in real-time, with its sensitivity comparable with other lesion imaging methods [63]. Though artifacts exist, such a problem may be solved shortly as multiple wavelengths and contrast agents are being developed [62]. Furthermore, it may not be a serious barrier for the penetration depth of PA method due to its adjustability of laser energy, fluence, and wavelength. Dana *et al.* also found that the small region between two lesion regions can also be clearly identified, emphasizing the capability of sPA to demonstrate regions where lesion continuity may be tough to identify by conventional methodologies [62]. As for in vivo application, given the recent advances in combined RFA-US catheter and the portable ways of intracardiac ablation, the development of a synthesis of an intracardiac probe being able to manipulate ablation and construct PA images at the same time is currently under way [64], [65]. PA imaging is also capable of monitoring the reversible temperature changes of cardiac tissue [66].

### B. CARDIOVASCULAR HEMODYNAMICS

Hemodynamic profile of the cardiovascular system is closely related to the risks and manifestations of cardiovascular diseases. Among various interacting factors, the hemoglobin concentration is one of the key elements. In 2004, Rinat *et al.* applied PA technique in monitoring total hemoglobin concentration [67]. Besides the potential to overcome limitations associated with traditional methods, PA technique also makes real-time identification of hemoglobin possible. Lesbo *et al.* has successfully performed the PA gas-rebreathing technique on the detection of compromised cardiac function in teenagers with pectus excavatum and found that PA technique correlates well with other conventional methods [68]. Other studies on the monitoring of oxygenation, total hemoglobin content and individual cells in blood have also shown a bright future of PAI application in the study of hemodynamics [69]–[71].

Several studies on the blood rheology have also demonstrated the triumphant prospect of PA technique in determining clinically relevant rheological parameters including hematocrit (Ht), RBC deformability (the ability of RBC to undergo deformation in flow), RBC aggregation and shear rates, and so on [72]–[76]. An in vivo study reported a high stage of sensitivity in dynamic rheological measurements in vessels using a combination of PA and photothermal (PT) methods [77]. Prior studies have shown that the increased PT/PA signal amplitude or a shortened rise time can result from the absence of radiative relaxation, which is dependent on the RBC of Hb state and properties of adjacent proteins [78]. Also, the spectrally optional optical excitation can provide information on RBC chemical features and composition, as the size and shape being associated with the processes of thermal relaxation [79]. Other studies have demonstrated that spectral imaging contrast may be amplified by the nonlinear effects of laser energy at high levels [51]. In summary, photoacoustic imaging based on PT/PA effects can be sensitive enough for the detection of changes in haemorheology with high accuracy and low artefacts.

Real-time imaging of cardiovascular dynamics can also be achieved by PAI technique. Taruttis *et al.* had demonstrated the real-time imaging of cardiovascular dynamics with multispectral optoacoustic tomography (MSOT), showing clear images including the aortic arch, carotid arteries, the anterior wall of the heart, and the adjacent structures such as the sternum, small blood vessels and part of the blood pools inside the ventricles [80]. Compared with the penetration capability of multi-photon microscopy (0.4-1 mm) or optical coherence tomography (<2 mm), PA imaging is capable of achieving a penetration depth of >10 mm, thus being able to visualize much deeper tissues [81]. Dean-Ben *et al.* performed a high-frame-rate four-dimensional optoacoustic tomography on heart perfusion and cardiac dynamics in a mouse model [82]. Due to the small size and quick heart rates (>400-600 bpm) in mice, traditional imaging methods including ultrasound and cardiac MRI are not qualified for cardiac function monitoring [83]–[87]. The frame rate of images can reach 50 per second, demonstrating 8 consecutive time points images acquired within one cardiac cycle of mouse [82]. The achievement in 3D demonstration with high accuracy and good imaging quality is more advanced compared to the 2D imaging systems, which are generally limited by the artefacts [88], [89]. Lihong V. Wang's team, by using stand-alone single-impulse panoramic photoacoustic computed tomography (SIP-PACT), which combined high spatiotemporal resolution (125 $\mu$m in-plane resolution, 50 $\mu$s per frame data acquisition and 50 Hz frame rate), deep penetration (48 mm cross-sectional width in vivo), with the use of anatomical, dynamical and functional contrasts, successfully imaged whole-body dynamics of living mice in a real-time manner and obtained clear sub-organ anatomical and functional details with full-view fidelity [90]. Moving along in application, in a proof-of-concept study, Smith *et al.* successfully used PAI-based real-time monitoring of systemic and microvascular mean oxygen saturation in a rat model of hypoxic shock [91]. A new PAI-based speckle tracking method was developed by de Hoop H *et al.*, which overcame the directional dependence and field-of-view limits of traditional Doppler imaging, and performed more accurately in various flow rates where ultrasound-based method fell short [92]. Recently, Zhang *et al.* proposed a PAI-based maneuver by obtaining data of vessel intensity and density of skin vasculature through in vivo imaging of animals under general anesthesia, which quantitatively correlated well with the greater blood perfusion, suggesting its potential clinical application of anesthesia monitoring [93].

### C. OTHERS

There are other variant forms of PAI applications in cardiovascular medicine. A dark-field PA microscopy was applied to allow more versatility in imaging, including to visualize the situation of the heart in real time, which may be of critical value during cardiac procedures and operations [94]. A high frequency (>25MHz) PA tomography built to view the blood flow in human fingers was another usage of this technique [95]. In a similar way, Park *et al.* reported the in vivo visualizing the blood flow to zebrafish heart [96]. And with the use of contrast agents made of single wall carbon nano-tubes (SWNT), the signals of PAI can be amplified [97], [98]. Mukaddim *et al.* utilized dual-wavelength PAI to monitor myocardial ischemia in mice by assessing variations in blood oxygen saturation, rendering it potentially feasible for real-time diagnosis and monitoring of cardiac ischemia. Using a hemispherical system, Lv *et al.* successfully delineated thoracic vessels and the entire heart in a murine model of acute myocardial infarction and was able to diagnose ischemic/infarct lesions up to 10mm in depth [99]. In light of these, PAI may also contribute to the identification and monitoring of cardiac ischemia and subsequent guidance of reperfusion therapy (or prevention of surgical damage). Another interesting application of PAI in cardiovascular medicine is the monitoring of anticoagulation. Using methylene blue as contrast agent, Wang *et al.* found a strong correlation between heparin concentration and photoacoustic signal, and then created a nanoparticle-based hybrid material as a wearable/implantable sensor of heparin [100].

## IV. FUTURE DIRECTIONS

In this review, we summarized all PAI applications used in various situations in cardiovascular medicine (Table 2). Specifically, compared with other modalities, PAI has been shown to be a relatively reliable technique to identify and evaluate atherosclerotic vulnerable plaques. Moreover, with its unique features, the applications of PAI technique is expandable also to other cardiovascular conditions.

Intravascular photoacoustic (IVPA) imaging, the catheter-borne version of PA imaging, is currently the most widely attempted application in preclinical studies aiming at characterizing atherosclerotic lesions. Previous studies in vulnerable plaque detection had largely focused on the

**TABLE 2.** Summary of current applications of photoacoustic imaging techniques in cardiovascular medicine.

| Clinical application | Imaging modality | Probe size | Probe characteristics | Image depth | Image axial resolution | Frame rate | Tissue target | Main results | Ref |
|---|---|---|---|---|---|---|---|---|---|
| Plaques | IVPA | 1.25 mm | IVPA: 1180 and 1230 nm | 1.4, 1.7 and 2.2 mm | None | 10 Hz | ex vivo, human coronary artery | Identification of lipid contents in vulnerable plaques. | [22] |
| | IVPA | None | IVPA: 1185 to 1235 nm | None | None | None | ex vivo, human coronary artery | Detection and differentiation of lipids in the atherosclerotic plaque and in peri-adventitial tissue. | [23] |
| | IVPA/IVUS | 2.2 mm | IVUS: 40 MHz IVPA: 1720nm | 2.5 mm | None | 10 Hz | in vivo ex vivo, rabbit aorta | The potential to visualize lipid deposits within the vessel wall and lumen. | [18] |
| | sIVPA/IVUS | 400 μm | IVPA: 1185 to 1235 nm | 1.2 μm: 5mm | None | 10 HZ | ex vivo, human coronary artery | Lipid detection in at 1.2 mm and 1.7 mm; differentiation between plaque and peri-adventitial lipids at 1.2 mm only. | [24] |
| | IVUS/IVPA | 600 μm | IVUS: 40 MHz IVPA: 730 to 830 nm | None | 22.5 mm | 10 HZ | Ex vivo, rabbit aorta | Detection of AuNRs within the arterial wall. | [31] |
| | IVPA | None | 530 nm 680 nm | None | None | 10 HZ | Ex vivo, rabbit aorta | Detection of macrophages in atherosclerotic plaques by plasmonic gold nanoparticles. | [30] |
| Plaques | IVUS/IVPA | 6F | IVUS: 40 MHz IVPA:1720 nm | None | None | 10 Hz | In vitro, rabbit aorta | Imaging of lipid in atherosclerotic plaques in the presence of luminal blood. | [16] |
| | MSOT | None | None | None | None | None | Human carotid plaque | Volumetric imaging of molecular probes (MMPSense-680) distributed deep within optically diffuse tissues. | [37] |
| | PAI | None | None | None | None | None | In vivo, rabbit aorta | The ability of AuNRs antibodies to enable quantitative detection of MMP2 in atherosclerotic plaques. | [38] |
| | Photo-acoustic compu-terized tomo-graphy scannerl | None | None | None | None | 5 MHz | In vivo, mice aorta | In vivo targeting and imaging of atherosclerosis by molecular probes ICG@PEG-Ag2S. | [43] |

**TABLE 2. (continued.) Summary of current applications of photoacoustic imaging techniques in cardiovascular medicine.**

| | | | | | | | | | |
|---|---|---|---|---|---|---|---|---|---|
| | IVUS-IVPA | 2.2 mm | IVUS: 45MHz IVPA: 800 nm | IVUS: 15 mm | None | 10 Hz | In vitro, porcine artery | Structural information and spatial distribution of ICG-labelled macrophages. | [44] |
| | IVUS-IVPA | 3.6 Fr | IVUS: 35 MHz IVPA: 532 mm | IVUS: 5 mm | IVUS: 59 mm | None | In vitro, rabbit aorta | IVPA better than IVUS in identifying the arterial wall. Resolution of IVPA at 35 MHz worse than at 80 MHz. | [45] |
| | IVUS-IVPA | 3.6 Fr | IVUS: 80 MHz IVPA: 532 mm | IVUS: 4 mm | IVUS: 35 mm | None | In vitro, rabbit aorta | | |
| | IVUS-IVPA | 8.7 Fr | IVUS: 35 MHz IVPA: 1197 mm | None | None | 1/s | In vitro, pig iliac artery | Detection of lipid-laden atherosclerotic plaque. | [46] |
| Arrhythmia | US-sPA | None | 740-780 nm | 3 mm | None | None | In vitro, Fresh porcine heart | Potential for assessment of RF ablation lesion size and position | [62] |
| Blood flow to the heart | US-PA | | Light weight ring-type transducer (0.38 g), inner diameter 3.5 mm, outer diameter 3.9 mm, height 7.6 mm | None | 38-42 μm | 28 | Zebrafish heart | In vivo visualization of blood flow of the zebrafish heart | [96] |
| Circulating clots | PT/PAFC | 5.5 mm in diameter | 530-600 nm | None | 12 μm | None | In vivo, human blood in vitro, mouse ear | Identification of white, red, and mixed clots | [50] |
| Blood rheology | PT/PAFC | 5.5 mm in diameter | None | None | None | None | In vivo, mouse model | Monitoring of multiple rheological parameters | [77] |

Notes: sPA – spectroscopic PA; MSOT – multispectral optoacoustic tomography; PAFC – PA flow cytometry; MMP – Matrix Metaloproteinase; AuNRs – Gold Nanorods

relationship between plaque pathology (i.e. plaque calcification, fibrous cap, and etc.) and patient symptoms. PAI, on the other hand, with its superior tissue specificity, is able to directly assess pathophysiological mechanisms associated with plaque vulnerability, including lipid distribution, inflammation, macrophage activity, intraplaque hemorrhage, and so on. However, there are also technical difficulties to be tackled with, including catheter composition with greater depth resolution and signal sensitivity, sheath material with less artefact generation or signal attenuation, stable platform for catheter rotation and data processing, and so on. Specifically, novel computational algorithms, when applicable, could possibly be borrowed from other disciplines, for instance, sparse Bayesian extreme learning machine [101]–[103], group-level brain functional network [104]–[107], and hybrid high-order functional connectivity networks [108], etc. In addition, the diagnostic performance of PAI in various pathological conditions, for example, bifurcation lesions, stent malapposition, in-stent thrombosis, and so on, remains unexplored.

Multi-modality imaging is frequently proposed to determinate plaque vulnerability for which a single technique can't meet the need of comprehensive assessment. On the one hand, PAI can be incorporated with other imaging technique to create a fusion system. A number of IVPA-IVUS or IVPA-OCT platforms are currently under development. On the other hand, tissue-specific targets/markers for the evaluation of inflammation or staging of atherosclerotic plaques in different animal models have become the point of interests for researchers. At present, the optimal procedures for such "enhanced" PAI application, and in particular, the choice of extraneous probes with their molecular targets, the route of

administration, the ideal technical parameters remain yet to be defined.

The application of PAI in non-atherosclerotic cardiovascular diseases often demonstrated only moderate results, in part due to the fact that most of these studies are but preliminary in nature. Monitoring of cardiac tissue during arrhythmia ablation procedures is proven feasible at least conceptually. Real-time modeling of cardiovascular hemodynamics, built on the PAI-based imaging of hemoglobin, seems to be the most promising application in this area. In general, this is another uncharted territory to be explored and calls for creative genius in science and engineering.

Still an emerging technology, PAI is in the phase of basic/translational research at the moment. With the integrated system being in the experimental stage, and its practical performance yet to meet the standards of clinical application, it might still take some time before the broad applications of PAI in cardiovascular medicine become fully materialized. Albeit premature to make any meaningful predictions, we believe that the unique advantages of PAI render it tremendously promising to open up new avenues in the study of cardiovascular diseases. It is our sincere hope that, in the not-too-distant future, PAI-based technologies will bring greater efficiency, accuracy and cost-effectiveness to the field of cardiovascular imaging.

## ACKNOWLEDGMENT

*(Da-Ya Yang, Yuan Zhu, and Jian-Qiu Kong contributed equally to this work.)*

## REFERENCES

[1] J. A. Schaar *et al.*, "Current diagnostic modalities for vulnerable plaque detection," *Current Pharmaceutical Des.*, vol. 13, no. 10, pp. 995–1001, 2007.

[2] F. Sharif and R. T. Murphy, "Current status of vulnerable plaque detection," *Catheterization Cardiovascular Intervent.*, vol. 75, no. 1, pp. 135–144, 2010.

[3] C. V. Bourantas *et al.*, "Hybrid intravascular imaging: Current applications and prospective potential in the study of coronary atherosclerosis," *J. Amer. College Cardiol.*, vol. 61, no. 13, pp. 1369–1378, 2013.

[4] C. V. Bourantas *et al.*, "Hybrid intravascular imaging: Recent advances, technical considerations, and current applications in the study of plaque pathophysiology," *Eur. Heart J.*, vol. 38, no. 6, pp. 400–412, 2017.

[5] T. Vo-Dinh, *Biomedical Photonics Handbook*. Boca Raton, FL, USA: CRC Press, 2003.

[6] S. Zackrisson, S. M. W. Y. van de Ven, and S. S. Gambhir, "Light in and sound out: Emerging translational strategies for photoacoustic imaging," *Cancer Res.*, vol. 74, no. 4, pp. 979–1004, 2014.

[7] K. Jansen, G. van Soest, and A. F. W. van der Steen, "Intravascular photoacoustic imaging: A new tool for vulnerable plaque identification," *Ultrasound Med. Biol.*, vol. 40, no. 6, pp. 1037–1048, 2014.

[8] B. Wang, J. L. Su, A. B. Karpiouk, K. V. Sokolov, R. W. Smalling, and S. Y. Emelianov, "Intravascular photoacoustic imaging," *IEEE J. Sel. Topics Quantum Electron.*, vol. 16, no. 3, pp. 588–599, May/Jun. 2010.

[9] E. Falk, P. K. Shah, and V. Fuster, "Coronary plaque disruption," *Circulation*, vol. 92, no. 3, pp. 657–671, 1995.

[10] J. A. Schaar, A. F. W. van der Steen, F. Mastik, R. A. Baldewsing, and P. W. Serruys, "Intravascular palpography for vulnerable plaque assessment," *J. Amer. College Cardiol.*, vol. 47, no. 8, pp. C86–C91, 2006.

[11] P. Libby, M. DiCarli, and R. Weissleder, "The vascular biology of atherosclerosis and imaging targets," *J. Nucl. Med.*, vol. 51, no. 1, pp. 33S–37S, 2010.

[12] R. Puri, E. M. Tuzcu, S. E. Nissen, and S. J. Nicholls, "Exploring coronary atherosclerosis with intravascular imaging," *Int. J. Cardiol.*, vol. 168, no. 2, pp. 670–679, 2013.

[13] P. D. Richardson, M. J. Davies, and G. V. R. Born, "Influence of plaque configuration and stress distribution on fissuring of coronary atherosclerotic plaques," *Lancet*, vol. 334, no. 8669, pp. 941–944, 1989.

[14] J. A. Schaar *et al.*, "Terminology for high-risk and vulnerable coronary artery plaques," *Eur. Heart J.*, vol. 25, no. 12, pp. 1077–1082, 2004.

[15] K. Jansen *et al.*, "Spectroscopic intravascular photoacoustic imaging of lipids in atherosclerosis," *Proc. SPIE*, vol. 19, no. 2, 2014, Art. no. 026006.

[16] B. Wang *et al.*, "Intravascular photoacoustic imaging of lipid in atherosclerotic plaques in the presence of luminal blood," *Opt. Lett.*, vol. 37, no. 7, pp. 1244–1246, 2012.

[17] A. Kole *et al.*, "Comparative quantification of arterial lipid by intravascular photoacoustic-ultrasound imaging and near-infrared spectroscopy-intravascular ultrasound," *J. Cardiovasc. Transl. Res.*, 2018. doi: 10.1007/s12265-018-9849-2.

[18] B. Wang *et al.*, "*In vivo* intravascular ultrasound-guided photoacoustic imaging of lipid in plaques using an animal model of atherosclerosis," *Ultrasound Med. Biol.*, vol. 38, no. 12, pp. 2098–2103, 2012.

[19] R. K. Al Dhahir, P. E. Dyer, and Z. Zhu, "Photoacoustic studies and selective ablation of vascular tissue using a pulsed dye laser," *Appl. Phys.*, vol. 51, no. 1, pp. 81–85, 1990.

[20] M. R. Price, T. F. Deutsch, M. M. Matthews-Roth, R. Margolis, J. A. Parrish, and A. R. Oseroff, "Preferential light absorption in atheromas *in vitro*," *J. Clin. Invest.*, vol. 78, no. 1, pp. 295–302, 1986.

[21] C.-L. Tsai, J.-C. Chen, and W.-J. Wang, "Near-infrared absorption property of biological soft tissue constituents," *J. Med. Biol. Eng.*, vol. 21, no. 1, pp. 7–14, 2001.

[22] K. Jansen, A. F. W. van der Steen, H. M. M. van Beusekom, J. W. Oosterhuis, and G. van Soest, "Intravascular photoacoustic imaging of human coronary atherosclerosis," *Opt. Lett.*, vol. 36, no. 5, pp. 597–599, 2011.

[23] K. Jansen, M. Wu, A. F. W. van der Steen, and G. van Soest, "Lipid detection in atherosclerotic human coronaries by spectroscopic intravascular photoacoustic imaging," *Opt. Express*, vol. 21, no. 18, pp. 21472–21484, 2013.

[24] K. Jansen, M. Wu, A. F. W. van der Steen, and G. van Soest, "Photoacoustic imaging of human coronary atherosclerosis in two spectral bands," *Photoacoustics*, vol. 2, no. 1, pp. 12–20, 2014.

[25] M. U. Arabul, M. Heres, M. C. M. Rutten, M. R. van Sambeek, F. N. van de Vosse, and R. G. P. Lopata, "Toward the detection of intraplaque hemorrhage in carotid artery lesions using photoacoustic imaging," *Proc. SPIE*, vol. 22, no. 4, 2017, Art. no. 041010.

[26] P. Libby, "Inflammation in atherosclerosis," *Nature*, vol. 420, no. 6917, pp. 868–874, 2002.

[27] J. S. Aaron *et al.*, "Plasmon resonance coupling of metal nanoparticles for molecular imaging of carcinogenesis *in vivo*," *Proc. SPIE*, vol. 12, no. 3, 2007, Art. no. 034007.

[28] K. Aslan, J. R. Lakowicz, and C. D. Geddes, "Plasmon light scattering in biology and medicine: New sensing approaches, visions and perspectives," *Current Opinion Chem. Biol.*, vol. 9, no. 5, pp. 538–544, 2005.

[29] J. Yguerabide and E. E. Yguerabide, "Resonance light scattering particles as ultrasensitive labels for detection of analytes in a wide range of applications," *J. Cellular Biochem.*, vol. 84, no. S37, pp. 71–81, 2001.

[30] B. Wang *et al.*, "Plasmonic intravascular photoacoustic imaging for detection of macrophages in atherosclerotic plaques," *Nano Lett.*, vol. 9, no. 6, pp. 2212–2217, 2009.

[31] D. E. Yeager *et al.*, "Intravascular photoacoustic imaging of exogenously labeled atherosclerotic plaque through luminal blood," *Proc. SPIE*, vol. 17, no. 10, 2012, Art. no. 106016.

[32] S. Link, C. Burda, M. B. Mohamed, B. Nikoobakht, and M. A. El-Sayed, "Laser photothermal melting and fragmentation of gold nanorods: Energy and laser pulse-width dependence," *J. Phys. Chem.*, vol. 103, no. 9, pp. 1165–1170, 1999.

[33] Y.-S. Chen *et al.*, "Enhanced thermal stability of silica-coated gold nanorods for photoacoustic imaging and image-guided therapy," *Opt. Express*, vol. 18, no. 9, pp. 8867–8878, 2010.

[34] Z. S. Galis, G. K. Sukhova, R. Kranzhöfer, S. Clark, and P. Libby, "Macrophage foam cells from experimental atheroma constitutively produce matrix-degrading proteinases," *Proc. Nat. Acad. Sci. USA*, vol. 92, no. 2, pp. 402–406, 1995.

[35] B. M. de Vries Wallis, J. L. Hillebrands, R. A. Tio, R. H. Slart, and C. J. Zeebregts, "Images in cardiovascular medicine. Multispectral near-infrared fluorescence molecular imaging of matrix metalloproteinases in a human carotid plaque using a matrix-degrading metalloproteinase-sensitive activatable fluorescent probe," *Circulation*, vol. 119, no. 20, pp. e534–e536, 2009.

[36] S. M. Yoon *et al.*, "Near-infrared fluorescence imaging using a protease-specific probe for the detection of colon tumors," *Gut Liver*, vol. 4, no. 4, pp. 488–497, 2010.

[37] D. Razansky *et al.*, "Multispectral optoacoustic tomography of matrix metalloproteinase activity in vulnerable human carotid plaques," *Mol. Imaging Biol.*, vol. 14, no. 3, pp. 277–285, 2012.

[38] H. Qin, Y. Zhao, J. Zhang, X. Pan, S. Yang, and D. Xing, "Inflammation-targeted gold nanorods for intravascular photoacoustic imaging detection of matrix metalloproteinase-2 (MMP2) in atherosclerotic plaques," *Nanomed., Nanotechnol., Biol. Med.*, vol. 12, no. 7, pp. 1765–1774, 2016.

[39] P. E. Stanga, J. I. Lim, and P. Hamilton, "Indocyanine green angiography in chorioretinal diseases: Indications and interpretation: An evidence-based update," *Ophthalmology*, vol. 110, no. 1, pp. 15–21, 2003.

[40] S. Yoneya, T. Saito, Y. Komatsu, I. Koyama, K. Takahashi, and J. Duvoll-Young, "Binding properties of indocyanine green in human blood," *Investigative Ophthalmol. Vis. Sci.*, vol. 39, no. 7, pp. 1286–1290, 1998.

[41] C. Zheng *et al.*, "Indocyanine green-loaded biodegradable tumor targeting nanoprobes for *in vitro* and *in vivo* imaging," *Biomaterials*, vol. 33, no. 22, pp. 5603–5609, 2012.

[42] C. Vinegoni *et al.*, "Indocyanine green enables near-infrared fluorescence imaging of lipid-rich, inflamed atherosclerotic plaques," *Sci. Transl. Med.*, vol. 3, no. 84, 2011, Art. no. 84ra45.

[43] C. Wu, Y. Zhang, Z. Li, C. Li, and Q. Wang, "A novel photoacoustic nanoprobe of ICG@PEG-$Ag_2S$ for atherosclerosis targeting and imaging *in vivo*," *Nanoscale*, vol. 8, no. 25, pp. 12531–12539, 2016.

[44] N. Q. Bui, K. K. Hlaing, Y. W. Lee, H. W. Kang, and J. Oh, "*Ex vivo* detection of macrophages in atherosclerotic plaques using intravascular ultrasonic-photoacoustic imaging," *Phys. Med. Biol.*, vol. 62, no. 2, pp. 501–516, 2017.

[45] X. Li, W. Wei, Q. Zhou, K. K. Shung, and Z. Chen, "Intravascular photoacoustic imaging at 35 and 80 MHz," *Proc. SPIE*, vol. 17, no. 10, 2012, Art. no. 106005.

[46] P. Wang *et al.*, "High-speed intravascular photoacoustic imaging of lipid-laden atherosclerotic plaque enabled by a 2-kHz barium nitrite Raman laser," *Sci. Rep.*, vol. 4, Nov. 2014, Art. no. 6889.

[47] S. Shang, Z. Chen, Y. Zhao, S. Yang, and D. Xing, "Simultaneous imaging of atherosclerotic plaque composition and structure with dual-mode photoacoustic and optical coherence tomography," *Opt. Express*, vol. 25, no. 2, pp. 530–539, 2017.

[48] W. Zhang *et al.*, "High-resolution, *in vivo* multimodal photoacoustic microscopy, optical coherence tomography, and fluorescence microscopy imaging of rabbit retinal neovascularization," *Light, Sci. Appl.*, vol. 7, Dec. 2018, Art. no. 103.

[49] E. J. Benjamin *et al.*, "Heart disease and stroke statistics-2017 update: A report from the american heart association," *Circulation*, vol. 135, no. 10, pp. e146–e603, 2017.

[50] E. I. Galanzha, M. Sarimollaoglu, D. A. Nedosekin, S. G. Keyrouz, J. L. Mehta, and V. P. Zharov, "*In vivo* flow cytometry of circulating clots using negative photothermal and photoacoustic contrasts," *Cytometry A*, vol. 79, no. 10, pp. 814–824, 2011.

[51] V. P. Zharov and V. S. Letokhov, *Laser Optoacoustic Spectroscopy*, 1st ed. Berlin, Germany: Springer-Verlag, 1986, p. 329.

[52] H. J. Jawad, M. Sarimollaoglu, A. S. Biris, and V. P. Zharov, "Dynamic blood flow phantom with negative and positive photoacoustic contrasts," *Biomed. Opt. Express*, vol. 9, no. 10, pp. 4702–4713, 2018.

[53] V. L. Roger *et al.*, "Heart disease and stroke statistics–2012 update: A report from the american heart association," *Circulation*, vol. 125, no. 1, pp. e220–e222, 2012.

[54] P. A. Wolf, R. D. Abbott, and W. B. Kannel, "Atrial fibrillation as an independent risk factor for stroke: The Framingham Study," *Stroke*, vol. 22, no. 8, pp. 983–988, 1991.

[55] P. A. Wolf, J. B. Mitchell, C. S. Baker, W. B. Kannel, and R. B. D'agostino, "Impact of atrial fibrillation on mortality, stroke, and medical costs," *Arch. Internal Med.*, vol. 158, no. 3, pp. 229–234, 1998.

[56] E. J. Benjamin, P. A. Wolf, R. B. D'Agostino, H. Silbershatz, W. B. Kannel, and D. Levy, "Impact of atrial fibrillation on the risk of death: The framingham heart study," *Circulation*, vol. 98, no. 10, pp. 946–952, 1998.

[57] B. J. Padanilam and E. N. Prystowsky, "Should atrial fibrillation ablation be considered first-line therapy for some patients? Should ablation be first-line therapy and for whom? The antagonist position," *Circulation*, vol. 112, no. 8, pp. 1223–1229, 2005.

[58] D. Shah, "A critical appraisal of cardiac ablation technology for catheter-based treatment of atrial fibrillation," *Expert Rev. Med. Devices*, vol. 8, no. 1, pp. 49–55, 2011.

[59] R. Cappato *et al.*, "Updated worldwide survey on the methods, efficacy, and safety of catheter ablation for human atrial fibrillation," *Circulat., Arrhythmia Electrophysiol.*, vol. 3, no. 1, pp. 32–38, 2010.

[60] C. P. Fleming, K. J. Quan, H. Wang, G. Amit, and A. M. Rollins, "*In vitro* characterization of cardiac radiofrequency ablation lesions using optical coherence tomography," *Opt. Express*, vol. 18, no. 3, pp. 3079–3092, 2010.

[61] S. A. Eyerly *et al.*, "Intracardiac acoustic radiation force impulse imaging: A novel imaging method for intraprocedural evaluation of radiofrequency ablation lesions," *Heart Rhythm*, vol. 9, no. 11, pp. 1855–1862, 2012.

[62] N. Dana, L. Di Biase, A. Natale, S. Emelianov, and R. Bouchard, "*In vitro* photoacoustic visualization of myocardial ablation lesions," *Heart Rhythm*, vol. 11, no. 1, pp. 150–157, 2014.

[63] J. G. Kim, M. Xia, and H. Liu, "Extinction coefficients of hemoglobin for near-infrared spectroscopy of tissue," *IEEE Eng. Med. Biol. Mag.*, vol. 24, no. 2, pp. 118–121, Mar./Apr. 2005.

[64] S. R. Dukkipati *et al.*, "The durability of pulmonary vein isolation using the visually guided laser balloon catheter: Multicenter results of pulmonary vein remapping studies," *Heart Rhythm*, vol. 9, no. 6, pp. 919–925, 2012.

[65] M. Wright *et al.*, "Real-time lesion assessment using a novel combined ultrasound and radiofrequency ablation catheter," *Heart Rhythm*, vol. 8, no. 2, pp. 304–312, 2011.

[66] G. A. Pang, E. Bay, X. L. Deán-Ben, and D. Razansky, "Three-dimensional optoacoustic monitoring of lesion formation in real time during radiofrequency catheter ablation," *J. Cardiovascular Electrophysiol.*, vol. 26, no. 3, pp. 339–345, 2015.

[67] R. O. Esenaliev, Y. Y. Petrov, O. Hartrumpf, D. J. Deyo, and D. S. Prough, "Continuous, noninvasive monitoring of total hemoglobin concentration by an optoacoustic technique," *Appl. Opt.*, vol. 43, no. 17, pp. 3401–3407, 2004.

[68] M. Lesbo *et al.*, "Compromised cardiac function in exercising teenagers with pectus excavatum," *Interact. Cardiovascular Thoracic Surg.*, vol. 13, no. 4, pp. 377–380, 2011.

[69] H. P. Brecht *et al.*, "*In vivo* monitoring of blood oxygenation in large veins with a triple-wavelength optoacoustic system," *Opt. Express*, vol. 15, no. 24, pp. 16261–16269, 2007.

[70] S. Hu, K. Maslov, and L. V. Wang, "Noninvasive label-free imaging of microhemodynamics by optical-resolution photoacoustic microscopy," *Opt. Express*, vol. 17, no. 9, pp. 7688–7693, 2009.

[71] I. Y. Petrova *et al.*, "Optoacoustic monitoring of blood hemoglobin concentration: A pilot clinical study," *Opt. Lett.*, vol. 30, no. 13, pp. 1677–1679, 2005.

[72] L. Dintenfass, "Blood rheology in cardio-vascular diseases," *Nature*, vol. 199, pp. 813–815, Aug. 1963.

[73] H. H. Lipowsky, "Microvascular rheology and hemodynamics," *Microcirculation*, vol. 12, no. 1, pp. 5–15, 2005.

[74] G. D. O. Lowe, "1 Blood rheology *in vitro* and *in vivo*," *Bailliére's Clin. Haematol.*, vol. 1, no. 3, pp. 597–636, 1987.

[75] G. Reggiori, G. Occhipinti, A. De Gasperi, J.-L. Vincent, and M. Piagnerelli, "Early alterations of red blood cell rheology in critically ill patients," *Crit. Care Med.*, vol. 37, no. 12, pp. 3041–3046, 2009.

[76] H. Schmid-Schönbein, "Blood rheology and physiology of microcirculation," *Ricerca Clin. Lab.*, vol. 11, pp. 13–33, 1981. [Online]. Available: https://www.ncbi.nlm.nih.gov/pubmed/7188106

[77] E. I. Galanzha and V. P. Zharov, "*In vivo* photoacoustic and photothermal cytometry for monitoring multiple blood rheology parameters," *Cytometry A*, vol. 79, no. 10, pp. 746–757, 2011.

[78] E. V. Shashkov, M. Everts, E. I. Galanzha, and V. P. Zharov, "Quantum dots as multimodal photoacoustic and photothermal contrast agents," *Nano Lett.*, vol. 8, no. 11, pp. 3953–3958, 2008.

[79] V. P. Zharov, "Far-field photothermal microscopy beyond the diffraction limit," *Opt. Lett.*, vol. 28, no. 15, pp. 1314–1316, 2003.
[80] A. Taruttis, E. Herzog, D. Razansky, and V. Ntziachristos, "Real-time imaging of cardiovascular dynamics and circulating gold nanorods with multispectral optoacoustic tomography," *Opt. Express*, vol. 18, no. 19, pp. 19592–19602, 2010.
[81] A. R. Mayer, J. M. Ling, A. B. Dodd, T. B. Meier, F. M. Hanlon, and S. D. Klimaj, "A prospective microstructure imaging study in mixed-martial artists using geometric measures and diffusion tensor imaging: Methods and findings," *Brain Imag. Behav.*, vol. 11, no. 3, pp. 698–711, 2017.
[82] X. L. Deán-Ben, S. J. Ford, and D. Razansky, "High-frame rate four dimensional optoacoustic tomography enables visualization of cardiovascular dynamics and mouse heart perfusion," *Sci. Rep.*, vol. 5, Jul. 2015, Art. no. 10133.
[83] R. Liao, B. K. Podesser, and C. C. Lim, "The continuing evolution of the Langendorff and ejecting murine heart: New advances in cardiac phenotyping," *Amer. J. Physiol.-Heart Circulatory Physiol.*, vol. 303, no. 2, pp. H156–H1567, 2012.
[84] M. Markl, P. J. Kilner, and T. Ebbers, "Comprehensive 4D velocity mapping of the heart and great vessels by cardiovascular magnetic resonance," *J. Cardiovascular Magn. Reson.*, vol. 13, p. 7, Jan. 2011.
[85] M. S. Maron, "Clinical utility of cardiovascular magnetic resonance in hypertrophic cardiomyopathy," *J. Cardiovascular Magn. Reson.*, vol. 14, no. 1, p. 13, 2012.
[86] M. S. Maron *et al.*, "Mitral valve abnormalities identified by cardiovascular magnetic resonance represent a primary phenotypic expression of hypertrophic cardiomyopathy," *Circulation*, vol. 124, no. 1, pp. 40–47, 2011.
[87] V. Mor-Avi *et al.*, "Current and evolving echocardiographic techniques for the quantitative evaluation of cardiac mechanics: ASE/EAE consensus statement on methodology and indications endorsed by the Japanese society of echocardiography," *Eur. J. Echocardiography*, vol. 12, no. 3, pp. 167–205, 2011.
[88] A. Buehler, X. L. Deán-Ben, D. Razansky, and V. Ntziachristos, "Volumetric optoacoustic imaging with multi-bandwidth deconvolution," *IEEE Trans. Med. Imag.*, vol. 33, no. 4, pp. 814–821, Apr. 2014.
[89] D. Queirós, X. L. Deán-Ben, A. Buehler, D. Razansky, A. Rosenthal, and V. Ntziachristos, "Modeling the shape of cylindrically focused transducers in three-dimensional optoacoustic tomography," *Proc. SPIE*, vol. 18, no. 7, 2013, Art. no. 076014.
[90] L. Li *et al.*, "Single-impulse panoramic photoacoustic computed tomography of small-animal whole-body dynamics at high spatiotemporal resolution," *Nature Biomed. Eng.*, vol. 1, no. 5, 2017, Art. no. 0071.
[91] L. M. Smith, J. Varagic, and L. M. Yamaleyeva, "Photoacoustic imaging for the detection of hypoxia in the rat femoral artery and skeletal muscle microcirculation," *Shock*, vol. 46, no. 5, pp. 527–530, 2016.
[92] H. de Hoop, H. Yoon, K. Kubelick, and S. Emelianov, "Photoacoustic speckle tracking for motion estimation and flow analysis," *Proc. SPIE*, vol. 23, no. 9, 2018, Art. no. 096001.
[93] X. Zhang, X. Qian, C. Tao, and X. Liu, "*In Vivo* imaging of microvasculature during anesthesia with high-resolution photoacoustic microscopy," *Ultrasound Med. Biol.*, vol. 44, no. 5, pp. 1110–1118, 2018.
[94] K. Maslov, G. Stoica, and L. V. Wang , "*In vivo* dark-field reflection-mode photoacoustic microscopy," *Opt. Lett.*, vol. 30, no. 6, pp. 625–627, 2005.
[95] T. Harrison, J. C. Ranasinghesagara, H. Lu, K. Mathewson, A. Walsh, and R. J. Zemp, "Combined photoacoustic and ultrasound biomicroscopy," *Opt. Express*, vol. 17, no. 24, pp. 22041–22046, 2009.
[96] J. Park *et al.*, "High frequency photoacoustic imaging for *in vivo* visualizing blood flow of zebrafish heart," *Opt. Express*, vol. 21, no. 12, pp. 14636–14642, 2013.
[97] H. Hong, T. Gao, and W. Cai, "Molecular imaging with single-walled carbon nanotubes," *Nano Today*, vol. 4, no. 3, pp. 252–261, 2009.
[98] M. Pramanik, K. H. Song, M. Swierczewska, D. Green, B. Sitharaman, and L. V. Wang, "*In vivo* carbon nanotube-enhanced non-invasive photoacoustic mapping of the sentinel lymph node," *Phys. Med. Biol.*, vol. 54, no. 11, pp. 3291–3301, 2009.
[99] J. Lv *et al.*, "Hemispherical photoacoustic imaging of myocardial infarction: *In vivo* detection and monitoring," *Eur. Radiol.*, vol. 28, no. 5, pp. 2176–2183, 2018.
[100] J. Wang *et al.*, "A nanoscale tool for photoacoustic-based measurements of clotting time and therapeutic drug monitoring of heparin," *Nano Lett.*, vol. 16, no. 10, pp. 6265–6271, 2016.
[101] H. Hosoya and A. Hyvärinen, "A mixture of sparse coding models explaining properties of face neurons related to holistic and parts-based processing," *PLoS Comput. Biol.*, vol. 13, no. 7, 2017, Art. no. e1005667.
[102] J. Luo, C.-M. Vong, and P.-K. Wong, "Sparse Bayesian extreme learning machine for multi-classification," *IEEE Trans. Neural Netw. Learn. Syst.*, vol. 25, no. 4, pp. 836–843, Apr. 2014.
[103] Q. Ye, H. Pan, and C. Liu, "A framework for final drive simultaneous failure diagnosis based on fuzzy entropy and sparse Bayesian extreme learning machine," *Comput. Intell. Neurosci.*, vol. 2015, 2015, Art. no. 427965. doi: 10.1155/2015/427965.
[104] M. Amboni *et al.*, "Resting-state functional connectivity associated with mild cognitive impairment in Parkinson's disease," *J. Neurol.*, vol. 262, no. 2, pp. 425–434, 2015.
[105] B. Jie, D. Zhang, W. Gao, Q. Wang, C.-Y. Wee, and D. Shen, "Integration of network topological and connectivity properties for neuroimaging classification," *IEEE Trans. Biomed. Eng.*, vol. 61, no. 2, pp. 576–589, Feb. 2014.
[106] Y.-B. Lee *et al.*, "Sparse SPM: Group sparse-dictionary learning in SPM framework for resting-state functional connectivity MRI analysis," *NeuroImage*, vol. 125, pp. 1032–1045, Jan. 2016.
[107] C.-Y. Wee, S. Yang, P.-T. Yap, and D. Shen, "Sparse temporally dynamic resting-state functional connectivity networks for early MCI identification," *Brain Imag. Behav.*, vol. 10, no. 2, pp. 342–356, 2016.
[108] Y. Zhang, H. Zhang, X. Chen, S.-W. Lee, and D. Shen, "Hybrid high-order functional connectivity networks using resting-state functional MRI for mild cognitive impairment diagnosis," *Sci Rep.*, vol. 7, no. 1, 2017, Art. no. 6530.

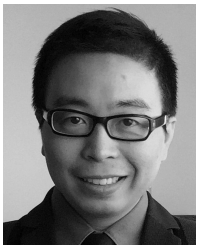

**DA-YA YANG** is currently an Attending Physician with the Department of Cardiology, The First Affiliated Hospital, Sun Yat-sen University, Guangzhou, China, and also with the NHC Key Laboratory of Assisted Circulation, Sun Yat-sen University.

He has co-authors several articles in the *International Journal of Cardiology*, *Canadian Journal of Cardiology*, *Cardiovascular Diabetology*, and so on.

**YUAN ZHU** is currently pursuing the master's degree with the Zhongshan School of Medicine, Sun Yat-sen University, Guangzhou, China.

She has co-authors several articles in the international journal *Parasitology Research* and so on.

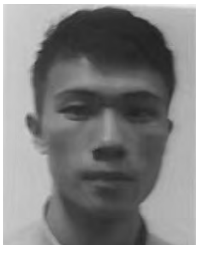

**JIAN-QIU KONG** is currently pursuing the master's degree with the Zhongshan School of Medicine, Sun Yat-sen University, Guangzhou, China.

He has co-authors several articles in the international journal *BMC Cancer* and so on.

**XIAO-JING GONG** is currently an Associate Research Fellow with the Research Laboratory for Biomedical Optics and Molecular Imaging, Shenzhen Institutes of Advanced Technology, Chinese Academy of Sciences, Shenzhen, China.

He has co-authors several articles in the *Journal of Biophotonics*, *Journal of Biomedical Optics*, *Nano-Micro Letters*, and so on.

**ZHI-HUA XIE** is currently an Assistant Research Fellow with the Research Laboratory for Biomedical Optics and Molecular Imaging, Shenzhen Institutes of Advanced Technology, Chinese Academy of Sciences, Shenzhen, China.

She has co-authors several articles in *Nano Letters*, *Optics Letters*, *Applied Physics Letters*, and so on.

**WEI-YI MEI** is currently a Deputy Chief Physician with the Department of Cardiology, The First Affiliated Hospital, Sun Yat-sen University, Guangzhou, China, and also with the NHC Key Laboratory of Assisted Circulation, Sun Yat-sen University.

He has co-authors several articles in the *Journal of Diabetes Investigation*, *Journal of Traditional Chinese Medicine*, *Heart, Lung and Circulation*, and so on.

**CHU-FAN LUO** is currently a Professor of medicine with the Department of Cardiology, The First Affiliated Hospital, Sun Yat-sen University, Guangzhou, China, and also with the NHC Key Laboratory of Assisted Circulation, Sun Yat-sen University.

He has co-authors several articles in the *Canadian Journal of Cardiology*, *Circulation: Cardiovascular Interventions*, *International Journal of Cardiology*, and so on.

**ZHI-MIN DU** is currently a Professor of medicine with the Department of Cardiology, The First Affiliated Hospital, Sun Yat-sen University, Guangzhou, China, and also with the NHC Key Laboratory of Assisted Circulation, Sun Yat-sen University.

He has co-authors several articles in *Atherosclerosis*, *Biochimica et Biophysica Acta*, the *Canadian Journal of Cardiology*, and so on.

**XIAO-DONG ZHUANG** is currently an Attending Physician with the Department of Cardiology, The First Affiliated Hospital, Sun Yat-sen University, Guangzhou, China, and also with the NHC Key Laboratory of Assisted Circulation, Sun Yat-sen University.

He has co-authors several articles in *Atherosclerosis*, *Biochimica et Biophysica Acta*, *Cellular Physiology and Biochemistry*, and so on.

**XIN-XUE LIAO** is currently a Professor of medicine with the Department of Cardiology, The First Affiliated Hospital, Sun Yat-sen University, Guangzhou, China, and also with the NHC Key Laboratory of Assisted Circulation, Sun Yat-sen University.

He has co-authors several articles in *Atherosclerosis*, *Biochimica et Biophysica Acta*, *Cellular Physiology and Biochemistry*, and so on.